

# Controlling the geometry and forces of a hybrid cable-net and fabric formwork for thin concrete shells

Diederik VEENENDAAL\*, Mile BEZBRADICA<sup>a</sup>, David NOVÁK<sup>b</sup>, Philippe BLOCK<sup>a</sup>

\*ETH Zurich, Institute of Technology in Architecture, BLOCK Research Group  
Stefano-Francini-Platz 5, HIL H 46.2, 8093 Zurich, Switzerland  
veenendaal@arch.ethz.ch

<sup>a</sup> ETH Zurich, Institute of Technology in Architecture, BLOCK Research Group

<sup>b</sup> ETH Zurich, Institute of Geodesy and Photogrammetry, Chair of Photogrammetry and Remote Sensing

## Abstract

The construction of anticlastic, thin-shell concrete structures can be efficiently achieved through the use of flexible formworks. Such formworks allow a departure from the traditional hyperbolic paraboloid shells, where its ruled surface serves as the basis for straight-line timber formworks. In addition, as forces are carried by the tensile system to the outer boundaries, the amount of falsework and their foundations, is heavily reduced, leading to economy in material, transportation and storage. This paper presents a prototype hybrid cable-net and fabric formwork used for the construction of two shell structures with identical boundary conditions. The second prototype, which is the main focus of this paper, was constructed after introducing several constructional variations and improvements. Moreover, it was constructed to test more accurate and flexible approaches to measuring both the geometry and internal forces of the cable net. This, in turn, allowed a higher degree of control of the applied prestresses, thus leading to lower tolerances between the digital form-finding model and the physical, as-built geometry.

**Keywords:** Shell structure, cable net, fabric formwork, flexible formwork, photogrammetry.

## 1. Introduction

Doubly curved, thin-shell concrete structures are structurally efficient systems for spanning large distances and covering large areas. However, their construction generally requires complicated custom timber or CNC-milled foam formworks with substantial scaffolding. An alternative concept is to use a flexible formwork (Veenendaal *et al.* [6]) for the construction of shells (Veenendaal & Block [5]).

Sections 1.1 and 1.2 explain the subject and context of the present research. Section 2 presents the problem statement and objective. Section 4 discusses the methods of measuring geometry and forces for two prototype shell structures, with results being presented in Section 5. A discussion and conclusion are given in Sections 6 and 7.

### 1.1. Hybrid cable-net and fabric formwork

By constructing a frame along the boundaries of a shell structure, and suspending or prestressing a cable net, a falsework for fabric shuttering is created. The resulting hybrid cable-net and fabric formwork is lightweight, easily transported, and allows unobstructed access underneath. Van Mele & Block [3, 4] presented a method for finding the distribution of forces required in such a cable net or stiffened membrane formwork to obtain a particular shape, after it has been loaded with fresh concrete. This control allows a range of pre-defined, non-analytical, anticlastic shapes to be designed and constructed. The use of a cable-net supported fabric was proposed by Zwartz & Jansma Architects to push the concept of a flexible formwork to the scale of long-span bridges (Torsing *et al.* [2]).

Two prototype shell structures were cast from a cable-net and fabric formwork (Figure 1). The first one was built as a constructional proof-of-concept and to develop an appropriate digital design process, while the second one was constructed to improve tolerances between computational model and physical result.



Figure 1: Sequence of construction of the first prototype, and the finished shell.

## 1.2. NEST HiLo

The experiments and prototype structures, presented in this paper, are intended to further inform and develop the design of the HiLo roof. HiLo is a research & innovation unit for NEST demonstrating ultra-lightweight construction. It is planned as a 16m×9m duplex penthouse apartment for visiting faculty of Empa and Eawag. NEST is a flagship project of Empa and Eawag in collaboration with the ETH Domain. It is a dynamic, modular research and demonstration platform for advanced and innovative building technologies on the Empa-Eawag campus in Dübendorf, Switzerland, to be completed in 2015 (Figure 2). As a “future living and working lab”, NEST consists of a central backbone and a basic grid to accommodate exchangeable living and office modules, such as HiLo, allowing novel materials and components, and innovative systems to be tested, demonstrated and optimized under real-world conditions. HiLo is a collaborative effort of the BLOCK Research Group and the Assistant Professorship of Architecture & Sustainable Technologies (SuAT), both at the Institute of Technology in Architecture, ETH Zurich, joined by Supermanoeuvre in Sydney as well as Zwarts & Jansma Architects (ZJA) in Amsterdam.

HiLo introduces several innovations, and this paper relates in particular to the development of a reusable and lightweight cable-net and fabric formwork system that allows the construction of the thin shell roof within acceptable tolerances.



Figure 2: Visualization of the preliminary design for NEST, with HiLo constructed at the top corner.

© EMPA and Gramazio & Kohler

## 2. Problem statement and objective

The geometry and tolerances of rigid formworks can simply be specified to a contractor. By contrast, the inherent flexibility of a cable-net and fabric formwork might pose issues for tolerances between the design and the as-built structure. The first prototype had an average deviation of 22mm, less than 1/100 of the span. The objective of the second prototype was to construct and prestress the formwork such that under loading of the fresh concrete, the resulting shape matches that of the original design, with a target value of 5mm set by the client, about 1/500 of the span.

### 3. Methodology

Two prototype shell structures were built reusing much of the same cable-net and fabric formwork. The target shape - the design - has straight edges, and slightly deviates from a hyperboloid. The midpoint is slightly higher which reduces maximum deflection. The bounding box of the shell is  $1.8\text{m} \times 1.8\text{m} \times 1.2\text{m}$ . Based on a uniform design thickness of 25mm, nodal target loads were calculated.

The process of designing these prototypes and calculating the initial prestresses is described in more detail by Veenendaal & Block [5], and included a best-fit form-finding procedure based on the work by Van Mele & Block [3,4]. Both prototypes were constructed and prestressed with turnbuckles, while continuously measuring the length of the cable segments with a tape measure.

Two different measuring strategies were applied to the prototypes, as explained in Section 4.1 and 4.2 and shown in Figure 3, both for measurement of geometry and forces. The resulting geometry after loading was then checked against the geometry of the design model.

	Geometry			Forces
	during prestressing	initial prestressed state	final loaded state	
<b>Prototype I</b>	tape measure	N/A	tape measure and laser metre (13)	springs (20)
<b>Prototype II</b>	tape measure	photogrammetry (60)	photogrammetry (60)	tension meter (140)

Figure 3: Equipment used for measuring geometry or forces in various stages for both prototypes (number of measurements in brackets).

#### 3.1. First prototype

In order to measure forces, the first cable net was fitted with springs (Federtechnik No. 50885.01) at 20 locations, one for each continuous cable. The springs were selected to have the highest (most sensitive) spring rate  $k$  while still fitting within the mesh of the cable net at maximum load.

The measured force  $F$  could then be calculated using Hooke's law, or  $F = k * u$ , where the spring rate  $k = 11.59\text{N/mm}$  according to the manufacturer and  $u$  is the measured elongation of the spring. Assuming a measuring error of  $\pm 1\text{mm}$ , the error in measured prestress  $F$  would be  $\pm 11.59\text{N}$ , or 4-12% full scale, given that the maximum prestresses were calculated to range between 93 and 262N.

Later, two reserve springs were load tested to check the specifications of the manufacturer. These showed that the actual spring rate varied between 13.4-24.0N/mm, exhibiting nonlinear behaviour for the first 15kg applied. This meant that in the end the accuracy was only between 40 and 50 % in our range.

After curing the concrete, the shell geometry was measured at 13 nodal points using a reference level  $z_0$ , tape measure for the horizontal position (x,y) and laser meter (Leica Disto Classic 5) for the vertical position (z) (Figure 4).



Figure 4: Measurement of first prototype; a Leica Disto Classic 5 laser metre for the geometry and springs for the forces.

### 3.2. Second prototype

To understand and control the relatively large differences between the actual and designed prestress states in the first prototype, the second prototype focused on alternative strategies to measure both force and geometry. Instead of springs, a compact and portable aircraft cable tension meter (Tensitron ACX-250-M, Figure 5) was used for the forces. When properly calibrated, it has an accuracy of 2% full scale (i.e. the error relative to the upper limit). With an upper limit of 250lbs, or 1,112N, this means an error of  $\pm 22.24\text{N}$ . This is more than the theoretical accuracy of the springs. However, the tension meter was assumed to be more reliable, faster, leaving no imprint on the concrete, and allowing a larger set of 140 measurements, one for each cable segment.

The loads from the wet concrete were simulated by discrete weights applied at the nodes, allowing access and transparency for both types of measurement. The loads were 1.5L PET bottles filled with sand, proportional to the tributary weight of each node, with an error of  $\pm 1\text{g}$  (Figure 5). The equivalent uniform thickness of the shell was modelled to be 15mm such that no more than one bottle per node was required. This meant a range of 1,545-2,146g per node, or an accuracy of 0.05-0.06% full scale.



Figure 5: Prestress introduced through twenty external turnbuckles, measured with a portable tension meter and applied loads from 60 sand-filled PET bottles.

Both the loaded and unloaded states were measured by photogrammetry at each of the 60 nodal points. The camera, a Nikon D3200 with a 20mm lens was calibrated using coded targets from the Australis Photometric package, thus allowing precise measurements of the nodal points. Afterwards, photographs were taken from a static platform, while rotating the model on the ground. Rotating the model allowed the three dimensional reconstruction of the nodal points while the camera is in the same position. The reconstruction was executed in the PhotoModeler Scanner application (Figure 6) and resulted in a point cloud model.

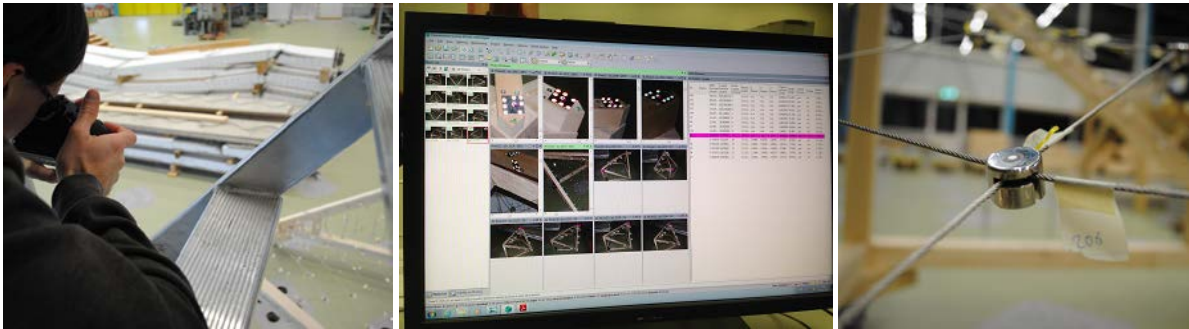


Figure 6: Measurement of second prototype; photogrammetry using a Nikon D3200 camera and PhotoModeler Scanner, and reference point on the nodal cross clamps for the geometry.

## 4. Results

The results from both prototypes were compared to the digital model.

### 4.1. First prototype

Measurements revealed an average deviation in vertical z-direction of 22.1mm with a standard deviation  $\pm 0.7$ mm. Unfortunately, this is far above the required 5mm tolerance. The deviation can be explained only in part by constructional tolerances and the error in the measurements. The main reason of the deviations is attributed to the assumed properties of the spring causing an accuracy of only 40-50% in the measured forces. The assumed cable stiffness and loads are both ruled out as major sources of inaccuracy.

- Varying the loads in the digital model equivalent to changes in uniform thickness of  $\pm 5$ mm, the position of the nodes varies by less than 1mm.
- For a higher E-modulus of  $210\text{kN/mm}^2$  (another common value for steel), forces differed no more than in the order of 0.1N (less than the accuracy of our measuring devices), and the maximum difference in cable length was in the order of  $1 \cdot 10^{-3}$ mm.

### 4.2. Second prototype

The point cloud data from photogrammetry was compared to the design model. Three comparisons were then made between the digital model and the as-built result (see Figure 8):

1. The distances between the resulting internal points and the nodes of the design model were calculated.
2. The boundary line of the edges did not exactly match that of the digital model, presumably due to construction tolerances and deformations of the timber frame. The digital model was therefore remapped to exactly fit the measured boundary. The distances were then calculated once more.
3. The measured nodes were projected to a mesh of the design model (approximating the target surface shape), to find corresponding closest points. The distance between the measurements and their projections were then calculated. Figure 7 explains the difference between comparison 2 and 3.

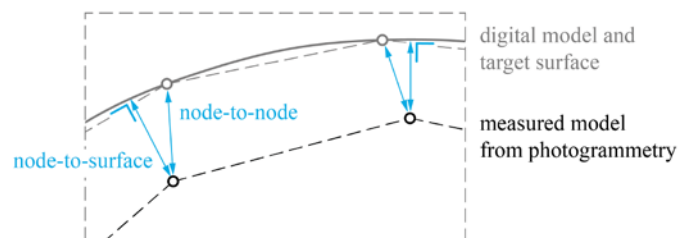


Figure 7: A comparison was made by measuring the distances from the measured points to the nodes of the digital model and to their projection onto the target surface.

These calculations were carried out for both the unloaded, prestressed state, and the final, loaded state. Figure 8 shows all three types of comparison for both states.

mean $\pm$ standard deviation, minimum to maximum [mm]	unloaded state	loaded state
<b>1 Node-to-node distance</b>	7.8 $\pm$ 2.5, 3.5 to 13.0	10.0 $\pm$ 2.6, 5.3 to 16.0
<b>2 Node-to-node distance, remapped boundaries</b>	7.0 $\pm$ 3.1, 1.1 to 14.2	7.0 $\pm$ 3.3, 1.6 to 15.0 (see Figure 9)
<b>3 Node-to-surface distance, remapped boundaries</b>	2.6 $\pm$ 1.4, 0.0 to 5.5	2.0 $\pm$ 1.5, 0.0 to 6.7

Figure 8: Three types of comparison between photogrammetric measurements and design model for both unloaded and loaded state.

Figure 9 shows the locations of turnbuckles, direction of assembling and prestressing the cable net. It also shows the asymmetry of the deviations (values for the second type of comparison, see Figure 8), with the largest deviations at the edge CD.

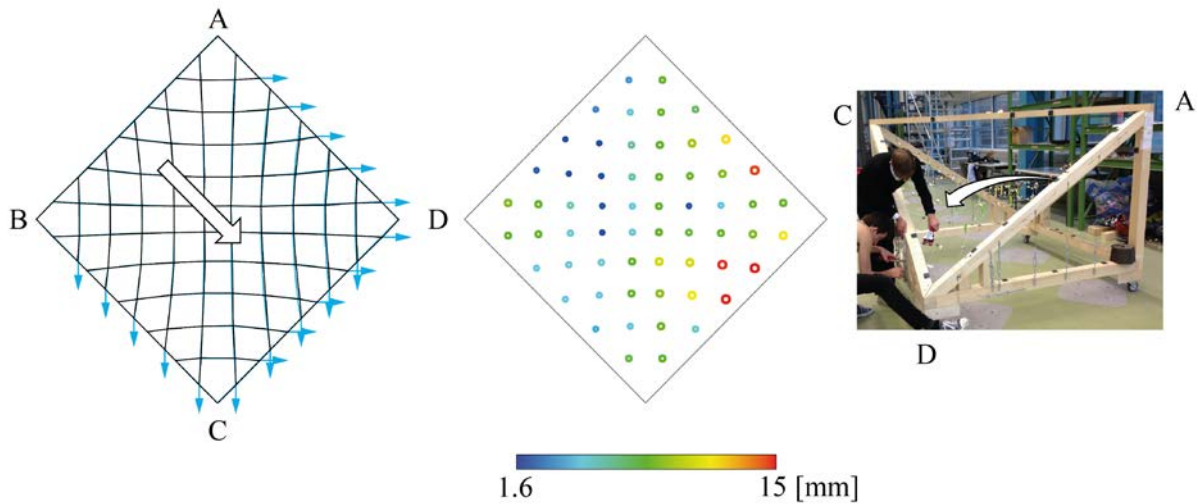


Figure 9: Position of turnbuckles (left), asymmetric distribution of deviations (middle), and direction of installing and prestressing the cable net (left and right).

Using measured forces  $F$  and lengths  $L$ , derived from the measured point coordinates in the loaded state, it is possible to calculate the force density  $Q = F/L$ . Using the force density method (Schek [1]), it is then possible to generate a geometry in static equilibrium using the same boundary conditions as the measured model and the measured force densities. Comparison of this geometry with that of the measurements is shown in Figure 10.

loaded state mean $\pm$ standard deviation minimum to maximum [mm]	compared to digital model (see also Figure 9)	compared to recomputed force density model
<b>node-to-node distance</b>	7.0 $\pm$ 3.3, 1.6 to 15.0	2.6 $\pm$ 1.0, 0.5 to 4.5
<b>node-to-surface distance</b>	2.0 $\pm$ 1.5, 0.0 to 6.7	1.3 $\pm$ 0.8, 0.0 to 3.1

Figure 10: Original comparison between as-built geometry and digital design model, and comparison between as-built geometry and geometry recalculated to be in static equilibrium

## 5. Discussion

An evaluation of the first prototype excluded modelling assumptions such as the loads and material stiffness as major sources of deviations in final construction.

Figure 8 shows that when conforming the digital design model to the measured boundary, the deviations are reduced relatively more in the loaded state than in the unloaded state. This suggests that deformation of the timber frame have a significant influence, and the edge points of the prototype cannot be considered to be fixed. Excluding this effect reduces the initial average deviation from 10mm to 7mm (-30%). Future formworks should therefore be designed to have boundary frames of higher stiffness, or be included in the form finding.

Figure 8 reveals that the in-plane deviations are higher than the out-of-plane deviations. The latter, the distances between the measured points and the target surface, are of greater interest when comparing structural behaviour of the as-built shell with that of the digital model. Arguably, they are also of greater importance for any client. The average deviation from the target surface is 2mm instead of the total of 7mm.

Figure 10 shows that the measured loaded state is not in static equilibrium. This suggests errors in measurements. Equilibrating the measured cable net, thus attempting to exclude measurement errors or variation in these measurements, reduces the average deviation from 7mm to 2.6mm (-44% of original 10mm). The average deviation from the target surface is then 1.3mm instead of 2.6mm. Further improvements on the measurements, especially of the forces, are therefore a priority if deviations are to be reduced even further.

Figure 9 visualizes the deviations, which show a correlation with the prestressing sequence. Turnbuckles were installed at one end of each continuous cable. The cable net was installed by placing nodes, measuring lengths and prestresses, while working from edge AB towards the opposite edge where the turnbuckles were. This will have introduced a cumulative error, explaining the asymmetry of the deviations. It is assumed that the remaining 2.6mm deviations (26% of original 10mm) are due to construction tolerances, with this asymmetry being the main cause. It is thus recommended to prestress in a symmetric fashion from both ends for future formworks and prefabricate or measure the cable net in such a way that cumulative errors are avoided.

Given the span of the shell of 2.546m, the average deviation over the span  $L$  can be argued to lie between  $1/255$  and  $1/1958$  of  $L$ . These tolerances are quite small, and in a general construction setting easily handled. Since measurements of force and geometry are possible at larger scales with the same or even better accuracy, similar tolerances should be achievable at full construction scale.

The present model has a relatively regular layout of the cables. For more complicated and asymmetric geometries, cable patterns and topologies, we may expect larger variations in the distribution of prestresses. Further work will clarify if and how this influences the accuracy of construction.



Figure 11: Final result of second prototype, loaded by first, second and fourth authors.

## 6. Conclusions

Two prototype shell structures were built and measured to determine the tolerances of hybrid cable-net and fabric formworks. The final result of the second prototype is shown in Figure 10.

The first prototype had an average deviation of 22.1mm, and the second only 10mm. By further excluding edge conditions and out-of-plane deviations, the deviation from the target surface was only 2.0mm. Compensating for

variation in measurements, the remaining average deviation ended up being only 1.3mm. Both prototypes serve as preliminary studies for a large shell structure to be built in 2015, and thus help to identify the most critical points of improvement, both for the digital modelling as the constructional approach to be undertaken for the final structure. Current tolerances are satisfactory, but recommendations for further improvement are stiffer edge conditions (or including them in the form finding), symmetric prestressing (from all cable ends), reducing cumulative errors when measuring cable-segment lengths and prestresses, and increasing accuracy of force measurements if possible.

## Acknowledgement

The authors would like to thank Jonas Sundberg for assistance with the prestressing and measuring of the second prototype, and Prof. Konrad Schindler for offering support on the photogrammetry and advising the third author.

## References

- [1] Schek H.-J., The force density method for form finding and computation of general networks. *Computer Methods in Applied Mechanics and Engineering*, 1974; **3**; 115-134.
- [2] Torsing R., Bakker J., Jansma R. and Veenendaal D., Large-scale designs for mixed fabric and cable-net formed structures, in *Proceedings of the 2nd international conference on flexible formwork*, Orr J. (ed.), 2012, 346-55.
- [3] Van Mele T., and Block P., A novel form finding method for fabric formwork for concrete shells, in *IASS 2010. Spatial Structures – Temporary and Permanent*, Zhang Q., Yang L. and Hu Y. (eds.), 2010.
- [4] Van Mele T. and Block P., Novel form finding method for fabric formwork for concrete shells. *Journal of the International Association of Shell and Spatial Structures*, 2011; **52**: 217-224.
- [5] Veenendaal D. and Block P., Design process for a prototype concrete shell using a hybrid cable-net and fabric formwork. *Engineering Structures*, 2014. Accepted for publication.
- [6] Veenendaal, D., West, M. and Block, P., History and overview of fabric formwork: using fabrics for concrete casting. *Structural Concrete - Journal of the fib*, 2011; **12**: 164-177.